

Version 1.0 as of June 22, 2009

Primary authors: The 1st generation LQ group

Comment to eno@umd.edu, rumerio@mail.cern.ch

Reply to EXO-008-010 by ****, 2009.

DRAFT

Grand unified theories [2], composite models [4], technicolor [3], as well as superstring-inspired E_6 models [5] are all well-motivated theories that postulate the existence of a symmetry, beyond the $SU(3)_C \times SU(2)_L \times U(1)_Y$ of the standard model (SM)[1], that relates quarks and leptons and that would imply the existence of new bosons, called leptoquarks (LQ). A LQ is colored, has fractional electric charge, can be spin 0 (scalar LQ) or spin 1 (vector LQ), and couples to a lepton and a quark with coupling strength λ . A LQ decays to a charged lepton and a quark (with unknown branching fraction β) or a neutrino and a quark (with branching fraction $1 - \beta$).

Constraints from experiments sensitive to flavor changing neutral currents, lepton family-number violation, and other rare processes[6] exclude LQ's with masses accessible to current collider experiments that couple to more than one quark/lepton generation. They also constrain the coupling constant λ at these masses to be less than 0.3.

This paper presents the results of a search for a first-generation LQ using a data sample corresponding to 50 pb^{-1} taken with the CMS detector during December, 2009 at the CERN LHC pp collider operating with $\sqrt{s}=10 \text{ TeV}$ using events containing two electrons and two jets. The peak instantaneous luminosity during this run was $2 \times 10^{32} \text{ cm}^{-2}\text{s}^{-1}$, corresponding to a mean number of pp interactions per crossing of 7 for a beam crossing time of 75 ns. Current limits from the CDF [7] and D0 experiments [8] constrain the mass of a first-generation scalar LQ to be $> 256 \text{ GeV}/c^2$.

In pp collisions at $\sqrt{s}=10 \text{ TeV}$, LQ's are predominantly pair-produced via gluon gluon fusion with a production cross section that is determined by the strong coupling constant α_s and that is independent of λ . The cross section depends on the spin and the mass of the LQ and has been calculated to NLO [9]. The uncertainty on the cross section is dominated by uncertainties on the parton distribution functions (PDF's) and has been estimated to be 10%. [10].

The CMS detector [15] consists of a large-bore superconducting solenoid with a 3.8T central field that encloses the central tracking and calorimeter systems. The central tracking system is composed of an all-silicon pixel and strip tracker that provide efficient reconstructions of vertices and the momenta of charged particles with pseudorapidities $|\eta| < 2.0$ [11]. A lead-tungstate scintillating-crystals electromagnetic calorimeter, and a brass-scintillator sampling hadron calorimeter are used to measure the momenta of photons, electrons, and hadrons. The central calorimeters cover $|\eta| < 1.4$ and the endcap calorimeters cover $|\eta| < 3.0$;

The iron yoke of the solenoid's flux-return is instrumented with four stations of muon detectors that cover $|\eta| < 2.4$. Forward sampling calorimeters extend the pseudorapidity coverage to high values ($\eta \approx 5$) assuring very good hermeticity. Luminosity is measured using the forward calorimeters. The normalization is set by a Van der Meer scan and the uncertainty is estimated to be 10%. [16]. Events that satisfy one of the trigger requirements are stored for offline analysis at a rate of approximately 100 Hz. Events first must pass a trigger from a system of fast electronics that reconstructs objects within a subsystem (calorimeter or muon) and that makes a decision for every beam crossing. The information from all subsystems for these events are then processed by a High Level Trigger (HLT) that consists of a farm of commercial cpu's that runs a version of the offline reconstruction optimized for timing considerations.

Events used in this analysis are required to pass a trigger that requires a cluster of energy in the electromagnetic calorimeter with $E_T > 10 \text{ GeV}/c$ and that passes a loose requirement on the ratio of hadronic to electromagnetic energy and shower shape requirements on the trigger tower in cluster containing the highest energy in the first level trigger and $15 \text{ GeV}/c$ in the HLT.

Electron candidates, reconstructed offline, are required to have a reconstructed electromagnetic cluster with transverse energy (E_T) $> 25 \text{ GeV}/c$, $|\eta| < 2.5$, and must be spatially matched to a reconstructed track in the central tracking system. (E_T is calculated using the energy from the calorimeter and angles from the matched track.) Electron candidates are further required to have a shower shape consistent with that of an electromagnetic shower and be isolated from other energy deposits in the calorimeter and from reconstructed tracks in the central tracking system. Only the two highest E_T electrons in the event are considered in this analysis. At least one of these two must be well-matched to the HLT electron that triggered the event. The energy scale is set using $Z \rightarrow ee$ and π_0 events. For electrons within the fiducial region of the calorimeter and with $E_T > 25 \text{ GeV}/c$, the average reconstruction efficiency is measured to be 95% by comparing the rate of $Z \rightarrow ee$ events, after background subtraction, with two electrons, and with only 1 electron, passing the full identification requirements. Due to a small gap between the barrel and endcap calorimeters at $|\eta| \approx 1.5$ and the reduced tracking efficiency beyond $|\eta|$ of 2.0, the efficiency times geometric acceptance for electrons is approximately 0.8. More details on the electron selection can be found in [17]

Jet are reconstructed from the calorimeter energies using an iterative cone algorithm. The jet energy scale is determined using a combination of dijet events and $pp \rightarrow \gamma + \text{jets}$ events. The jet energy resolution is measured using dijet events. More details on the jet reconstruction and calibration can be found in [18]. Jets that are within a cone of size $\Delta R = \sqrt{\Delta(\eta^e - \eta^j)^2 + \Delta(\phi^e - \phi^j)^2} = 0.3$ of one of the two highest E_T electrons passing the ID requirements are removed from the jet list. In this analysis, only jets with $E_T > 25$ GeV/ c and $|\eta| < 3.0$ are considered. Only the two highest E_T jets are used in the subsequent analysis.

Muons are used as part of our data-based evaluation of backgrounds from standard model processes. Muons candidates are constructed from a track reconstructed in the central tracking system with a good match to a reconstructed track in the muon system. Muons used in this analysis are required to have transverse momentum (P_T) > 25 GeV/ c and $|\eta| < 2.0$. The muon reconstruction efficiency is measured in data using $Z^0 \rightarrow \mu^+ \mu^-$ events.

We select an initial sample containing two electrons and two jets. The dominant SM processes that produce such events are $t\bar{t}$ and $Z \rightarrow ee + \text{jets}$ production. Other backgrounds include multijet production with at least 2 jets misidentified as electrons, W+jets events with a jet mis-identified as an electron, and multi-boson production. To reduce these backgrounds, we require both electrons have $E_T > 30$ GeV/ c , and both jets have $E_T > 50$ GeV/ c . To reduce the background from $Z \rightarrow ee$ production, we require the invariant mass of the electrons to be > 100 GeV/ c^2 . To further reduce all SM backgrounds, we require S_T , defined as the scalar sum of the magnitudes of the P_T of the electrons and jets. The value of the S_T requirement depends on the LQ mass and is given in table I. The cut value was chosen as the one that is predicted to give the optimum signal significance.

The acceptances times efficiency for pair-production of scalar LQ's is given in Tab. I, and is evaluated using Monte Carlo LQ events produced with the PYTHIA[12] event generator and a detector simulation based on GEANT[13], overlaid with events collected by the CMS detector without any trigger requirement (to simulate the effects of other pp collisions in the same crossing and detector noise). A small correction ($O(x\%)$) to $e \cdot A$ is applied based on the electron identification efficiencies measured using $Z \rightarrow ee$ events and jet resolutions measured using dijet events.

The $t\bar{t}$ background is evaluated both using MC (MADGRAPH [14] plus full detector simulation) and using a data-based technique. Since the W's produced in $t\bar{t}$ events decay to

mass (GeV/ c^2)	S_T cut	LQ A	LQ A · e	number events
250	XX	XX	XX	XX
350	XX	XX	XX	XX
450	XX	XX	XX	XX
550	XX	XX	XX	XX

TABLE I: Acceptance (A) for $LQ\overline{LQ}$ events to pass the geometric and kinematic requirements of this analysis, acceptance times efficiency (A·e) for passing the electron and jet identification requirements, and number of events expected in 50 pb^{-1} .

electrons and muons, while LQ decay's are constrained to only one generation, events that pass all the LQ selection requirements, except with one electron and one muon instead of two electrons, can be used to estimate this background. The background in the two electron sample is given by

$$B_{t\bar{t}} = 0.5 N_{e\mu} \frac{e \cdot A(ee)_{MC}}{e \cdot A(e\mu)_{MC}}$$

where $e \cdot A$ is the acceptance for $t\bar{t}$ events as evaluated using the full MC corrected for the data-derived efficiencies and resolutions. We observe XXX events in our control sample for an S_T requirement of 460 GeV, for a statistical uncertainty on our background prediction of XX%. The two methods give similar results.

The $Z \rightarrow ee$ background is also evaluated using both MC (MADGRAPH plus full detector simulation) and using a data-based method. For the data-based method, we select events passing all the LQ selection requirements, but reversing the M_{ee} requirement. The predicted background is then

$$B_{Z \rightarrow ee} = N_{M_{ee} < 100}^{data} \frac{N_{M_{ee} > 100}^{MC}}{N_{M_{ee} < 100}^{MC}}$$

. We observe XXX events in our control sample for an S_T requirement of 460 GeV, for a statistical uncertainty on our background prediction of XX%. Both methods give similar results.

The multijet background is evaluated from the data using a sample of events with four reconstructed jets with $E_T > 25 \text{ GeV}/c$ and passing all LQ selection requirements, but with S_T calculated using the sum of the jet E_T 's. The number of events is multiplied by the

Cut	LQ(350)	$t\bar{t}$	$Z \rightarrow ee$	other B	Data
Trigger and Skim	XX	XX	XX	XX	xX
e and jet P_T and η requirements	XX	XX	XX	XX	xx
$M(ee) > 100 \text{ GeV}/c^2$	XX	XX	XX	XX	xx
$S_T > 400 \text{ GeV}$	XX	XX (xx)	XX (xx)	XX	xx

TABLE II: Predicted numbers of events as selection requirements are added for 50 pb^{-1} of pair production of a $350 \text{ GeV}/c^2$ LQ with $\beta = 1$, $t\bar{t}$ production, $Z \rightarrow ee$ +jets production, and other backgrounds (B), along with the number of events observed in data. For the backgrounds, the first number is the predicted number of events from the MC, while the number in parentheses is the prediction from the data-based method.

probability for a jet to fake an electron, measured in γ +jet data. This background is negligible.

The rest of the backgrounds are evaluated using MC.

The predicted and measured number of events after each set of requirements is given in Tab. II for an S_T requirement of 460 GeV. The number of events in the data are in good agreement with the background-only hypothesis. In addition, the kinematic distributions also agree well. Figure 1 shows the electron-jet mass from data, predicted backgrounds and for the signal. There are two entries per event; the electron-jet pairing that minimizes the mass difference between the e^+ -jet and the e^- -jet invariant masses is used.

For setting upper limits in the absence of the leptoquark signal, the Bayesian approach[20] is used, with systematic uncertainties marginalized as nuisance parameters. The systematic uncertainties for the backgrounds are dominated by the number of events in the control samples. Systematic uncertainties on the signal include (in order of importance) the uncertainty on the integrated luminosity ($\pm 10\%$), uncertainties on the production cross section ($\pm 10\%$), jet energy scale, electron identification efficiencies.

Limits as a function of β are given in Figure 2 along with the expected limit. As you can see, our limit is worse than expected, and we may expect interesting things in the future.

In conclusion, we have presented search for first-generation LQ. Our data is in good agreement with the expectations from SM processes. Our limit on the mass of a scalar

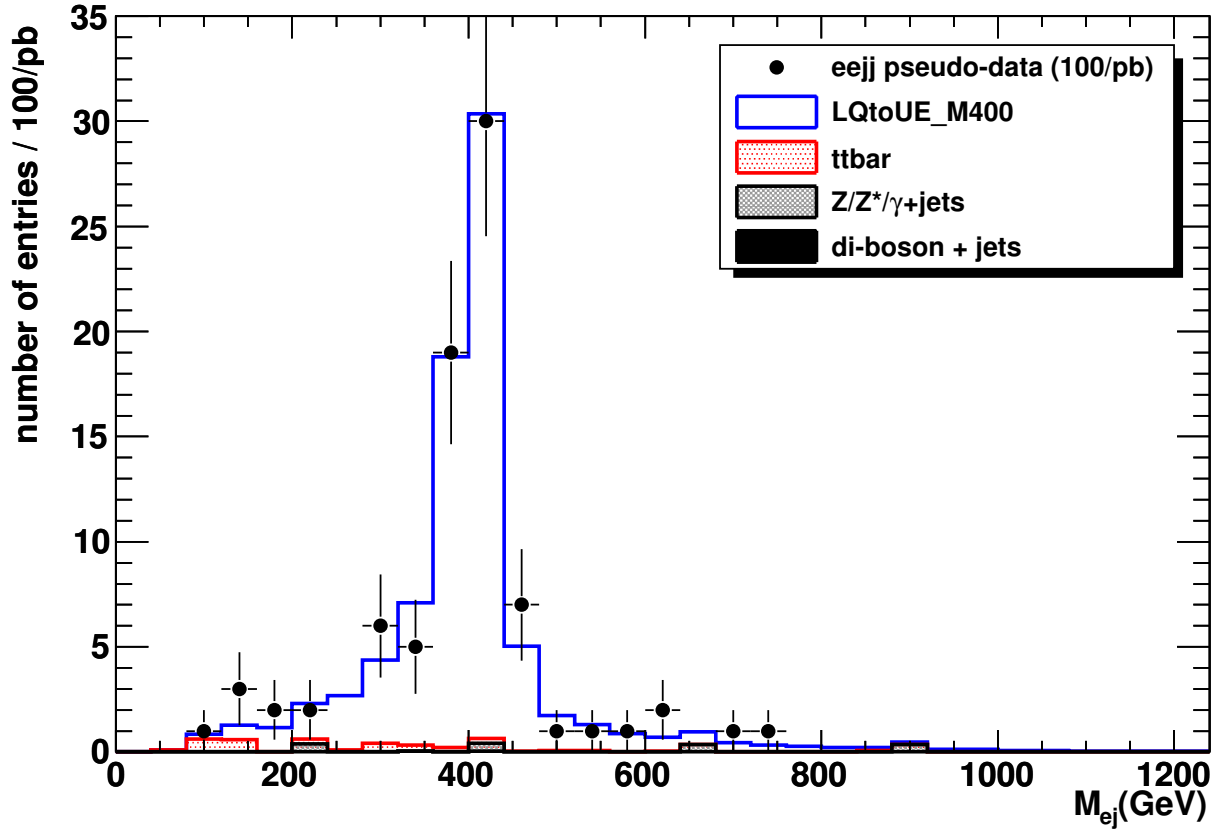


FIG. 1: Invariant mass of the LQ and the $\bar{L}Q$ candidates in events with two electrons and two jets (points) with prediction from SM background sources (lines). The electron-jet pairing that gives the minimum difference between the two candidates is used.

leptoquark with $\beta = 1$ is $535 \text{ GeV}/c^2$.

We thank the technical and administrative staff at CERN and other CMS Institutes, and acknowledge support from: FMSR (Austria); FNRS and FWO (Belgium); CNPq, CAPES, FAPERJ and FAPESP (Brazil); MES (Bulgaria); CERN; CAS, MST and NSFC (China); MST (Croatia); RPF (Cyprus); Academy of Sciences and NICPB (Estonia); Academy of Finland, ME and HIP (Finland); CEA and CNRS/IN2P3 (France); BMBF, DFG and HGF (Germany); GSRT and Leventis Foundation (Greece); OTKA and NKTH (Hungary); DAE and DST (India); IPM (Iran); SFI (Ireland); INFN (Italy); KICOS (Korea); CINVESTAV, CONACYT, SEP and UASLP-FAI (Mexico); PAEC (Pakistan); SCSR (Poland); FCT (Portugal); JINR (Armenia, Belarus, Georgia, Ukraine, Uzbekistan); MST and MAE (Russia); MSD (Serbia); MCINN and CPAN (Spain); Swiss Funding Agencies (Switzerland); NSC

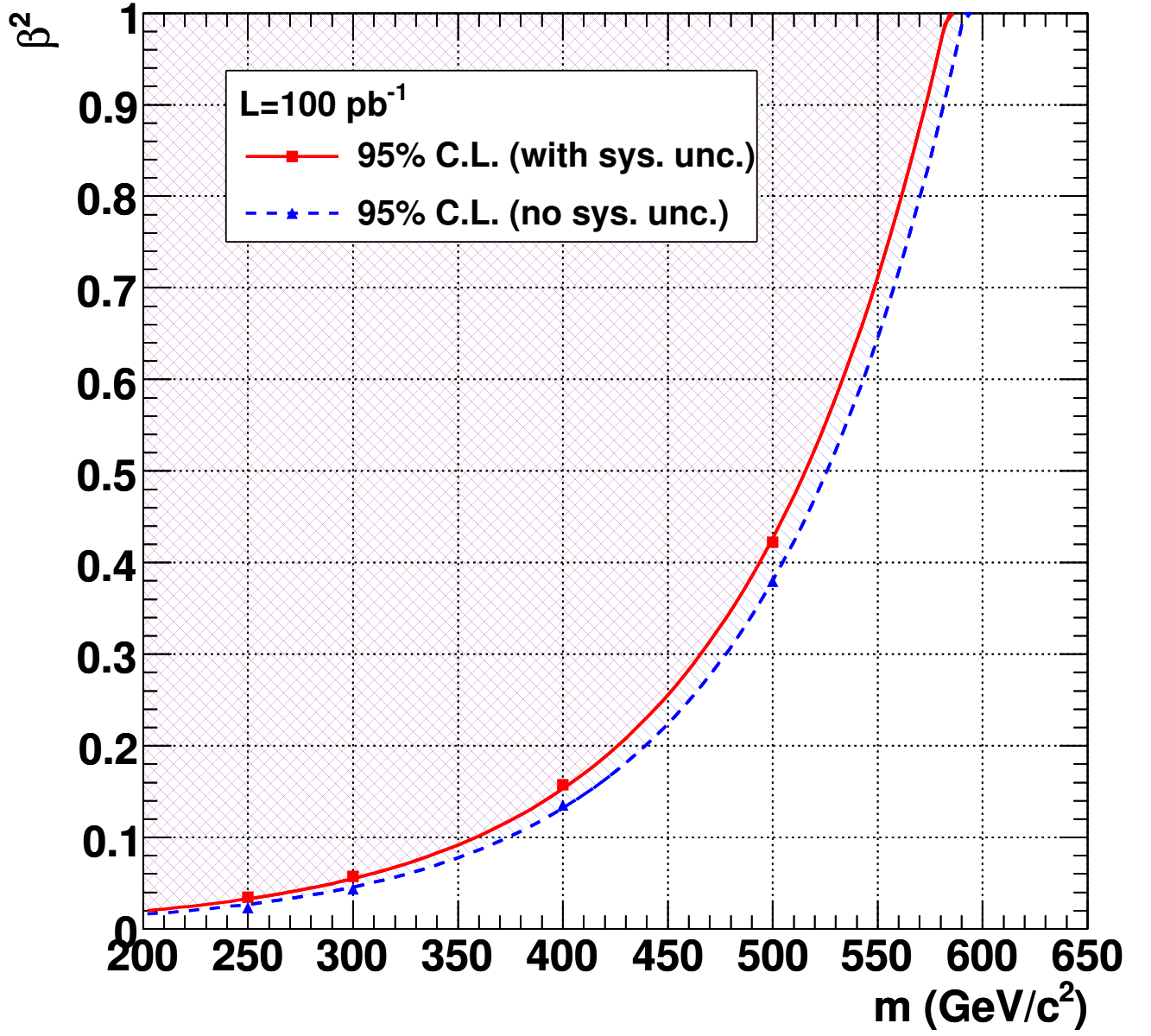


FIG. 2: Observed and expected 95% confidence-level limit on the mass of a first-generation scalar LQ as a function of the LQ branching fraction to an electron and a jet, β .

- [1] S. Glashow, Nucl. Phys. **22**, 579 (1961); S. Weinbert, Phys. Rev. Lett. **19**, 1264 (1967); A. Salam, in *Elementary Particle Theory*, edited by N. Svartholm (Almqvist and Wiksells, Stockholm, 1969), p. 367; W. Bardeen, H. Fritzsch, and M. Gell-Mann, in *Scale and Conformal Symmetry in Hadron Physics*, edited by R. Gatto (Wiley, New York, 1973), p. 139; D. Gross and F. Wilczek, Phys. Rev. D **8**, 3633 (1973); S. Weinbert, Phys. Rev. Lett. **31**, 494 (1973).
- [2] J.C. Pati and A. Salam, Phys. Rev. D **10**, 275 (1974).
- [3] S. Dimopoulos and L. Susskind, Nucl. Phys. B **155** (1979); S. Dimopoulos, Nucl. Phys. B **168** (1980); E. Eichten and K. Lane, Phys. Lett. B **90** (1980).
- [4] W. Buchmuller and D. Wyler, Phys. Lett. B **177**, 377 (1986).
- [5] V.D. Angelopoulos *et al.*, Nucl. Phys. B **292** (1987).
- [6] W. Buchmuller, R. Ruckl, and D. Wyler, Phys. Lett. B **191**, 442 (1987); **448**, 320(e) (1999).
- [7] D. Acosta *et al.* [CDF Collaboration], Phys. Rev. D **72**, 051107 (2005).
- [8] V.M. Abazov *et al.* [D0 Collaboration], Phys. Rev. D **71**, 071104(R) (2005).
- [9] M. Kramer, arXiv:0411038.
- [10] M. Kramer, private communication.
- [11] CMS uses a cylindrical coordinate system with the z axis running along the beam axis. The angles θ and ϕ are the polar and azimuthal angles, respectively. Pseudorapidity is defined as $\eta = -\ln[\tan(\theta/2)]$ where θ is measured with respect to the interaction vertex. In the massless limit, η is equivalent to the rapidity $y = (1/2)\ln[(E + p_z)/(E - p_z)]$.
- [12] pythia reference
- [13] Application Software Group, CERN Program Library Long Writeup, W5013.
- [14] madgraph reference
- [15] S. Chatrchyan *et al.*, JINST **3** S08004.
- [16] paper on luminosity determination
- [17] paper on cms electron id
- [18] paper on cms jet id
- [19] paper on cms muon id
- [20] C. Amsler *et al.*, Physics Letters B **667**, 1 (2008), section 32.3.1.